Electrochemical Biosensing in Cancer Diagnostics and Follow-up

Maria Freitas,[a] Henri P. A. Nouws,*[a] and Cristina Delerue-Matos[a]

Abstract: In cancer, screening and early detection are critical for the success of the patient's treatment and to increase the survival rate. The development of analytical tools for non-invasive detection, through the analysis of cancer biomarkers, is imperative for disease diagnosis, treatment and follow-up. Tumour biomarkers refer to substances or processes that, in clinical settings, are indicative of the presence of cancer in the body. These biomarkers can be detected using biosensors, that, because of their fast, accurate and point of care applicability, are prominent alternatives to the traditional methods. Moreover, the constant innovations in the biosensing field improve the determination of normal and/or elevated levels of tumour biomarkers in patients' biological fluids (such as serum, plasma, whole blood, urine, etc.). Although several biomarkers (DNA, RNA, proteins, cells) are known, the detection of proteins and circulating tumour cells (CTCs) are the most commonly reported due to their approval as tumour biomarkers by the specialized entities and commonly accepted for diagnosis by medical and clinical teams. Therefore, electrochemical immunosensors and cytosensors are vastly described in this review, because of their fast, simple and accurate detection, the low sample volumes required, and the excellent limits of detection obtained. The biosensing strategies reported for the six most commonly diagnosed cancers (lung, breast, colorectal, prostate, liver and stomach) are summarized and the distinct phases of the sensors' constructions (surface modification, antibody immobilization, immunochemical interactions, detection approach) and applications are discussed.

Keywords: cancer biomarker • electrochemical biosensing • immunosensor • cytosensor • nanomaterial

1 Introduction

The International Agency for Research on Cancer (IARC) estimated that in 2012 there were 14.1 million new cancer cases, 8.2 million cancer deaths and 32.6 million people living with cancer (within 5 years of diagnosis) worldwide [1].

According to the World Health Organization (WHO) cancer is a generic term for a large group of diseases that can affect any part of the body. The major feature of cancer is the rapid creation of abnormal cells that grow beyond their usual boundaries, and can then spread to other organs, a process referred to as metastasis, which is the major cause of death from cancer [2].

The most commonly diagnosed cancers in 2012 were lung (1.82 million), breast (1.67 million), colorectal (1.36 million), prostate (1.1 million cases), stomach (951000 cases) and liver (782000 cases). These six cancers represent 55 per cent of the global incidence burden in 2012 [1].

When cancer is present in the body the levels of several substances can be altered both in or on tumour cells as well as in biological fluids (blood, urine, etc.). These substances are produced by cancer cells or by other cells of the body in response to cancer or certain benign (noncancerous) conditions [3] and are referred to as biomarkers. This includes abnormalities in DNA (germline or somatic), RNA, proteins, metabolites, and abnormal cellular or tissue processes. A particular cancer type can be detected through qualitative and/or quantitative analysis of a certain biomarker [4]. These biomarkers may also be used to monitor the response to treatment and allow patient follow-up. The identification of circulating (peripheral blood) biomarkers, analysed in so called "liquid biopsies", would have enormous implications in diagnosis and treatment [5] and avoid the traditional invasive biopsy.

2 Cancer Biomarkers

Currently, a wide range of specific biomolecules has been proposed as potential biomarkers for cancer detection. However, the vast majority still need to be validated for use in the clinical setting, mainly because of lack of specificity and/or sensitivity. Protein biomarkers can be detected in distinct cancer stages and are classified as prognostic, therapeutic or diagnostic biomarkers. The screening and evaluation of an individual's susceptibility to cancer can contribute and support the decisions of medical teams, underlying the risk of incidence or progression. The detection is normally conducted in bio-

[a] M. Freitas, H. P. A. Nouws, C. Delerue-Matos
REQUIMTE/LAQV, Instituto Superior de Engenharia do Porto, Politécnico do Porto, Rua Dr. António Bernardino de Almeida, 4200-072 Porto, Portugal
E-mail: han@isep.ipp.pt

logical fluids, with serum being the most desirable testing matrix in clinical tests. This non-invasive practise has revitalized early detection [6].

The electrochemical analysis of circulating protein biomarkers is the main focus of this review because of their potential prognostic value. However, a detailed description of these biomarkers is beyond the scope of this review and the authors' expertise. Therefore, a short summary of the common protein biomarkers used for the development of electrochemical immunosensors related to the six most commonly diagnosed cancers in 2012 is presented in Table 1.

Table 1. Some protein cancer biomarkers.

Cancer	Protein Biomarker	Ref
Lung	Neuron-Specific Enolase (NSE)	[14–19] [20–22]
	Squamous Cell Carcinoma antigen (SCC)	
Breast	Human epidermal growth factor receptor 2 (HER2)	[23–30]
	Cancer Antigen 15-3 (CA 15-3)	[31–39]
Colorectal and Stomach	Cancer Antigen 19-9 (CA 19-9)	[40–43]
Prostate	Prostate-Specific Antigen (PSA)	[44–69]
Liver	α-1-Fetoprotein (AFP)	[70–99]
Stomach	Cancer Antigen 72-4 (CA 72-4)	[100–101] [102]
	Interleukin-6 (IL-6)	

(i) Lung cancer, the most incident cancer-type with the highest cancer mortality rate worldwide, is mainly divided into two broad categories: small-cell lung carcinoma (SCLC) and non-small cell lung carcinoma (NSCLC). Neuron specific enolase (NSE) is a specific protein marker in lung cancer detection and a high percentage of patients with SCLC have elevated serum NSE concentrations at diagnosis. On the other hand, cytokeratin fragment 21-1 (CYFRA 21-1), squamous cell carcinoma antigen (SCC) and carcinoembryonic antigen (CEA) have been associated with NSCLC cases, which represent the vast majority of lung cancer cases [7]; (ii) Breast cancer is a healthcare concern of women worldwide. The protein biomarkers with evidence of clinical utility for breast cancer include CEA, Human epidermal growth factor receptor 2 (HER2) and Cancer Antigen 15-3 (CA 15-3) [8]; (iii) Colorectal cancer (CRC) is the second most commonly diagnosed cancer among women and third among men worldwide. Two of the most widely known serum protein biomarkers for CRC are the Cancer Antigen 19-9 (CA 19-9) and CEA. Simultaneous detection of both biomarkers is beneficial in evaluating the therapeutic effect [9]; (iv) Prostate cancer is the most common cancer-type in men. Prostate specific antigen (PSA) is the classic and the most widely used protein biomarker for clinical diagnosis [10]; (v) Hepatocellular carcinoma (HCC) is the fifth most common cancer, representing more than 90% of primary liver cancer, and is frequently detected by α-fetoprotein (AFP). Nevertheless, three serum biomarkers are normally suggested to determine the risk of liver cancer: AFP, AFP-L3, and des-gamma-carboxy-prothrombin (DCP) [11]; (vi) Stomach cancer, also known as gastric cancer, remains one of the leading challenges in oncologic research because of its frequent occurrence and poor prognosis. Besides the

classical serum-based protein biomarkers associated with stomach cancer (CEA, CA 19-9 and Cancer Antigen 72-4 (CA 72-4)), the interleukin IL6 is also considered a valuable biomarker for this type of cancer [12].

As referred previously, several classic biomarkers are eligible for cancer diagnosis. However, a careful and judicious decision is often necessary to avoid false results and thus a misdiagnosis. The simultaneous (multiplexed) detection of distinct biomarkers could avoid these problems. For example, CEA leads to effective cancer detection, but is non-specific (it is commonly used to monitor several cancer types, such as colorectal, lung, gastric, pancreas, liver and breast) So, its overexpression only indicates the presence of an elevated amount of cancer cells [13]. Therefore, the combination of CEA and other more specific biomarkers can greatly contribute to a more reliable diagnosis.

Throughout this review the state of the art of electrochemical immunosensors and immunoassays in the field of cancer analysis is discussed. Besides this, because of the large number of recent developments related to circulating tumor cells (CTCs), the detection of these cells using electrochemical devices is also included. For the selected analytical strategies included in this work the actual design, construction and detection approach are analysed and discussed. The most relevant topics related to the recently published electrochemical sensors are presented in summarized tables.

3 Electrochemical Biosensors

The established tests to determine cancer biomarkers are based on invasive methods, such as biopsies, followed by immunohistochemistry (IHC) and fluorescent in situ hybridization (FISH) analysis methods [103]. Although the detection of protein cancer biomarkers in blood or serum is not a routine practice, their analysis is possible and is mainly based on enzyme-linked immunosorbent assays (ELISA). However, some of these assays are not sufficiently sensitive for the detection of low biomarker concentrations [104] and in the prognostic detection, which is then susceptible to produce false results [105].

To overcome this problem major efforts have been made to develop more sensitive analytical techniques for biomarker detection, with a special emphasis on biosensors. The International Union of Pure and Applied Chemistry (IUPAC) defines a biosensor as “an integrated receptor-transducer device, which is capable of providing selective quantitative or semi-quantitative analytical information using a biological recognition element” [106]. The biological recognition element can be DNA, an antibody, an antigen, an enzyme, a whole cell, a cell organelle, etc. The transducer is used to covert the recognition event into an analytically useful signal. This signal transduction can be based on electrochemical, optical, piezoelectric and calorimetric principles. Biosensors are usually designed to provide highly selective and sensitive detection of target analytes through the use of specific biological recognition elements combined with highly sensitive detection techniques. Among the several types of biosensors, the ones that employ electrochemical detection (voltammetry, amperometry, potentiometry, conductometry and electrochemical impedance spectroscopy) are the most widely studied. Electrochemical biosensors are outstanding candidates for inclusion in portable (point-of-care) systems because, besides their fast responses, simplicity and ease of use, the instrumentation needed to perform the analysis has been reduced to (low-cost) pocket-size dimensions. Furthermore, after the development of individual assays for the biomarkers, their combination to form multiplexed detection systems is possible. Therefore, they can provide fast recording of biomarker tumour profiles, which can play an important role in early diagnosis and personalized medicine.

4 Electrochemical Immunosensors for Protein Cancer Biomarker Analysis

Most of the electrochemical biosensors developed to date for the detection of cancer protein biomarkers are voltammetric or amperometric immunosensors. Therefore, only these types of sensors are included in this review. Furthermore, because of the large amount of published studies and the extension of this review, only a reduced number of these articles can be presented. The studies included were retrieved from the Clarivate Analytics Web of Science database (timespan: 2007–2017) by combining the following keywords: cancer, protein biomarker, biosensor and electrochemistry. Although studies without the application in real samples were excluded, a few studies in which these samples were not used were included because of the interest of the construction of the sensing phase or the detection label.

A summary of electrochemical immunosensors (EI) for the analysis of protein biomarkers of lung (Table 2), breast (Table 3), colorectal and stomach (Table 4), prostate (Table 5), liver (Table 6) and stomach (Table 7), cancer is presented. This summary focuses on several important features of the sensors: the transducer electrode and its surface modification, the immobilization strategy of the capture antibody, the assay type, the electrochemical detection technique, the species detected, the sample, and the limit of detection (LOD).

Promising new strategies have been implemented in the design and construction of immunosensors for early screening and cancer diagnosis. Voltammetric and amperometric sensors are especially interesting because of the high sensitivity that can be attained. Electrochemical biomarker detection has been carried out with distinct techniques (amperometry, cyclic voltammetry (CV), linear sweep voltammetry (LSV), differential pulse voltammetry (DPV), square wave voltammetry (SWV), stripping voltammetry and electrochemical impedance spectroscopy (EIS)). Amperometry, CV and DPV are the most commonly employed techniques because they provide low

Table 2. Lung cancer biomarker analysis with electrochemical immunosensors.

Biomarker	Transducer	Surface modification	Immobilization	Assay	Label	Technique	Detection	Sample	LOD	Ref.
NSE	GCE	Hydrogel/Gold nanoparticles (AuNP)	Adsorption	Label-free	n/a	SWV	$[Fe(CN)_6]^{3-/4-}$	Patient serum	0.26 pg/mL	[14]
	GCE	Thionine (TH)/Carbon nanosphere-functionalized graphene	Adsorption	Sandwich	Platinum nanoflower (PtNF)-labeled horseradish peroxidase (HRP)	DPV	H_2O_2	Spiked new-born cattle serum	5.0 pg/mL	[15]
	GCE	β-Cyclodextrin (CD)	Affinity	Sandwich	Guanine-decorated graphene nanostructures (GGN)	DPV	$Ru(NH_3)_6^{3+}$	Spiked new-born cattle serum	1.0 pg/mL	[16]
	GCE	Single-walled carbon nanotubes (SWCNTs)	Covalent (EDC/NHS)	Competitive	n/a	DPV	1-NP	Patient serum	33 pg/mL	[17]
	GCE	Gold nanocrystals (AuNC)/nickel hexacyanoferrate nanoparticles/Gold nanoparticle (AuNP)-functionalized graphene nanosheets (GS)	Adsorption	Label-free	n/a	CV	$[Fe(CN)_6]^{3-/4-}$	Patient serum	0.3 pg/mL	[18]
	GCE	Prussian blue (PB)-silica dioxide/3-aminopropyltriethoxysilane (APTES)/ Chitosan (CS)-AuNP	Adsorption	Label-free	n/a	CV	PB	Patient serum	80 pg/mL	[19]
SCC	GCE	Nitrogen-doped graphene sheets (N-GS)	Covalent (GA)	Sandwich	Sodium montmorillonites/polyaniline/AuNPs	Amperometry	H_2O_2	Human serum	0.33 pg/mL	[20]
	GCE	Reduced graphene oxide (rGO)-tetraethylene pentamine (TEPA)	Covalent (GA)	Sandwich	Gold-silver nanoclusters	Amperometry	H_2O_2	n/a	1.3 pg/mL	[21]
	GCE	N-GS	Covalent (GA)	Sandwich	Dumbbell-like Pt-Fe_3O_4 NPs	Amperometry	H_2O_2	Human serum	15.3 pg/mL	[22]

1-NP: 1-naphthol; CV: Cyclic voltammetry; DPV: Differential pulse voltammetry; EDC: 1-ethyl-3-(3-dimethylaminopropyl)-carbodiimide; GA: Glutaraldehyde; GCE: Glassy Carbon Electrode; H_2O_2: Hydrogen Peroxide; NHS: N-hydroxysuccinimide; NSE: Neuron-Specific Enolase; PB: Prussian blue; SCC: Squamous Cell Carcinoma antigen; SWV: Square wave voltammetry.

Table 3. Breast cancer biomarker analysis with electrochemical immunosensors.

Biomarker	Transducer	Surface modification	Immobilization	Assay	Label	Technique	Detection	Sample	LOD	Ref.
HER2	8×SPE	Streptavidin MBs (Strep-MBs) Protein A-MBs (ProtA-MBs) Streptavidin MBs (Strep-MBs)	Affinity	Sandwich	AP	DPV	1-NP	Spiked human serum	1.8 ng/mL 2.6 ng/mL 3.4 ng/mL	[23]
	CILE	Multi-walled carbon nanotubes (MWCNT)/Gold nanoparticles (AuNPs)	Adsorption	Label-free	n/a	EIS	1-NP	Patient serum	7.4 ng/mL	[24]
	GSPE	AuNPs	Adsorption	Label-free	n/a	EIS	$[Fe(CN)_6]^{3-/4-}$	Spiked human serum	6.0 ng/mL	[25]
	SPCE	–	Covalent (EDC/NHS)	Sandwich	HRP	Amperometry	HQ	Human cells lysates	1.0 µg/mL	[26]
	SPCE	AuNPs	Adsorption	Sandwich	AP	LSV	Silver	Spiked human serum	4.4 ng/mL	[27]
	AuE	AuNP/3-Mercaptopropionic acid (MPA)/Cysteamine/Fe_3O_4 NPs	Covalent (2-iminithiolane)	Label-free	n/a	DPV	$[Fe(CN)_6]^{3-/4-}$	Patient serum	0.995 pg/mL	[28]
	SPCE	Magnetic beads-Protein A (MBs-Protein A)	Affinity (Protein A)	Sandwich	AP	DPV	1-NP	Patient serum	6.0 ng/mL	[29]
	Au-NEEs	Polycarbonate	Adsorption	Sandwich	HRP	CV	MB	Cell lysates	n/a	[30]
CA 15-3	AuE	Cys/Graphene oxide (GO)/Py	Covalent (EDC/NHS)	Sandwich	MWCNT-Ferritin	DPV	HQ	Spiked human serum	0.009 U/mL	[31]
	GCE	Ionic liquid (IL)-functionalized GS	Covalent (EDC/NHS)	Sandwich	Cd^{2+}-functionalized nanoporous TiO_2	SWV	Cadmium	n/a	0.008 U/mL	[32]
	ITO	Graphene oxide (GO)	Affinity interaction (Avidin)	Sandwich	Tyrosinase (Tyr)	Chronocoulometry	o-Benzoquinone	Spiked human serum	0.100 U/mL	[33]
	GCE	AuNP/ferrocene (Fc)-rGO	Adsorption	Label-free	n/a	DPV	Fc	Patient serum	0.015 U/mL	[34]
	GCE	Nitrogen-doped graphene sheets (N-GS)	Covalent (EDC/NHS)	Label-free	n/a	DPV	$[Fe(CN)_6]^{3-/4-}$	Spiked human serum	0.012 U/mL	[35]
	GCE	Nanoporous gold/Gra/TH	Covalent (GA)	Sandwich	HRP-encapsulated liposomes	DPV	TH	Patient serum	5×10^{-6} U/mL	[36]
	GCE	CNTs-OrgSi@CS/PtNCs/GOD	Adsorption	Label-free	n/a	CV	$FADH_2$	Spiked human serum	0.040 U/mL	[37]
	AuE	Ferrocenecarboxylic (Fc-COOH)-doped silica nanoparticles (SNPs)	Covalent (GA)	Label-free	n/a	CV	Fc-COOH	Patient serum	0.640 U/mL	[38]
	AuE	PB/AuNP/dsDNA/AuNP	Adsorption	Label-free	n/a	CV	PB	Patient serum	600 pg/mL	[39]

1-NP: 1-naphthol; 8× SPE: eight screen-printed electrochemical cells; AuE: Gold electrode; AP: Alkaline phosphatase; CA 15-3: Cancer Antigen 15-3; CILE: carbon ionic liquid electrode; CV: Cyclic voltammetry; DPV: Differential pulse voltammetry; EDC: 1-ethyl-3-(3-dimethylaminopropyl)-carbodiimide; EIS: Electrochemical impedance spectroscopy; Fc: ferrocene; GA: Glutaraldehyde; GCE: Glassy carbon electrode; GSPE: Graphite screen-printed electrodes; HER2: Human epidermal growth factor receptor 2; HQ: Hydroquinone; HRP: Horseradish peroxidise; ITO: Indium-tin oxide; LSV: linear sweep voltammetry; MB: Methylene blue; NEEs: Nanoelectrode ensembles; NHS: N-hydroxysuccinimide; PB: Prussian blue; SPCE: Screen-printed carbon electrode; SWV: Square wave voltammetry; TH: Thionine.

Table 4. Colorectal and Stomach cancer biomarker analysis with electrochemical immunosensors.

Biomarker	Transducer	Surface modification	Immobilization	Assay	Label	Technique	Detection	Sample	LOD	Ref.
CA 19-9 (Colorectal and Stomach)	SPCE	Chitosan	Covalent (GA)	Sandwich	AuNP/poly (amidoamine) dendrimer (PAAD)	Amperometry	H_2	Patient serum	0.0063 U/mL	[40]
	GCE	AuNPs-porous GO	Adsorption	Sandwich	Au@Pd-Gra/TH/HRP	DPV	TH	Patient serum	0.006 U/mL	[41]
	GCE	CS/MWCNTs/glucose oxidase/silica-protected magnetite particle-Gold-mesoporous silica (Fe_3O_4@SiO_2–Au@mSiO_2)	Adsorption	Label-free	n/a	DPV	Glucose oxidase (GOD)	n/a	0.004 U/mL	[42]
	AuE	MWCNTs-BSA/gold colloids	Adsorption	Sandwich	Nafion coated SiO_2 NPs	CV	$[Fe(CN)_6]^{3-/4-}$	Patient serum	0.060 U/mL	[43]

AuE: Gold electrode; CA 19-9: Cancer Antigen 19-9; CV: Cyclic voltammetry; DPV: Differential pulse voltammetry; GA: Glutaraldehyde; GCE: Glassy carbon electrode; HRP: Horseradish peroxidise; SPCE: Screen-printed carbon electrode; TH: Thionine.

limits of detection (LOD), in the order of pg/mL and/or fg/mL, for the cancer biomarkers reported in this review.

Voltammetric and amperometric sensors generally incorporate a three-electrode configuration, composed of working-, reference- and auxiliary electrodes, which are placed in contact with the sample. Then the potential of the working electrode (WE) is either varied within a predefined potential range (voltammetry) or fixed at a constant potential (amperometry) and the resulting current is measured. The analytical process thus occurs at the WE and therefore the recognition element is immobilized on the surface of this electrode. The WE is a small-size electrode or a screen-printed electrode (SPE) made of, for example, carbon, gold, or platinum. Other specific working electrodes such as indium tin oxide (ITO) or paper electrodes [33,53] are also employed depending on the specifications or characteristics of the electrochemical technique and the biosensor performance. Moreover, the WE can be modified with nanostructures and distinct materials such as carbon nanotubes, gold nanoparticles, nanoelectrode ensembles (NEEs) prepared in track-etched polycarbonate membranes [30], a multiwalled carbon nanotube-ionic liquid (MW-CILE) [24], and a three-dimensional Au nanowire array (3D AuNW) with electropolymerized polypyrrole [55].

5 Electrode Surface Modification

Sensor surfaces modified with nanostructures can provide an additional increment in the biosensor's performance and advanced development of portable devices that can support early cancer diagnosis [107]. The WE′s surface is therefore frequently modified with (nano) materials such as metal (especially gold) nanoparticles or nanocomposites and carbon nanostructures to (i) improve the immobilization and the stability of the biological recognition element, (ii) increase the recognition element's load, (iii) enhance the sensor's sensitivity and/or (iv) change the detection potential to minimize interferences of other species. For the last two purposes, a redox mediator can also be included in the surface modification strategy.

Gold nanoparticles (AuNP) are an excellent nanomaterial with favourable biocompatibility, good conductivity, and a high surface-to-volume ratio. As examples of sensors using AuNPs, Ravalli et al. [25] developed a sensitive biosensor based on easy immobilization of the bioreceptor on AuNPs, electrodeposited on screen-printed graphite. Marques et al. [27] used screen-printed carbon electrodes, modified with AuNPs, for effective antibody immobilization. In this work, the formation of the AuNPs was achieved through electrodeposition of ionic gold by applying a constant current followed by applying a constant potential. Chu et al. [48] used AuNPs as a substrate material to immobilize the antibodies and to accelerate electron transfer. The AuNPs were prepared in accordance with the conventional citrate method that consists of reducing the gold nanoparticles with a

Table 5. Prostate cancer biomarker analysis with electrochemical immunosensors.

Biomarker	Transducer	Surface modification	Immobilization	Assay	Label	Technique	Detection	Sample	LOD	Ref.
PSA	GCE	Graphene/CoS–Au	Adsorption	Sandwich	Toluidine blue/CeO_2 mesoporous nanoparticles/ionic liquids doped carboxymethyl chitosan (TB/M–CeO2/CMC/ILs)	DPV Amperometry	TB H_2O_2	Spiked human serum	0.16 pg/mL	[44]
	GCE	Sulfo group functionalized multi-walled carbon nanotubes/Gold NP (MWCNTs-SO_3H@Au)	Adsorption	Sandwich	Mesoporous core-shell Pd@Pt NP-amino group functionalized graphene (M–Pd@Pt/NH_2-GS)	Amperometry	H_2O_2	Spiked human serum	3.3 fg/mL	[45]
	AuE	CD/p-Toluenesulfonyl chloride (PTSC)/ethylenediamine	Covalent (GA)	Label-free	n/a	DPV	$[Fe(CN)_6]^{3-/4-}$	Human serum	0.3 pg/mL	[46]
	GCE	Graphene sheets-APTES@AuNPs (GS-APTES@Au)	Adsorption	Sandwich	APTES-cubic Cu_2O-ferrocene-carboxylic acid (APTES-Cu_2O@Fc-COOH)	DPV	H_2O_2	Spiked human serum	0.05 pg/mL	[47]
	GCE	AuNPs	Adsorption	Sandwich	Palladium-doped cuprous oxide nanoparticles (Pd@Cu_2O NPs)	Amperometry	H_2O_2	Spiked human serum	2.0 fg/mL	[48]
	8X SPCE	Streptavidin-MBs	Affinity (Streptavidin/Biotin)	Sandwich	HRP	Amperometry	TMB	Patient serum	1.86 ng/mL	[49]
	GCE	High molecular-weight silk peptide/ Reduced graphene oxide (rGO)	Covalent (GA)	Label-free	n/a	DPV	$[Fe(CN)_6]^{3-/4-}$	Patient serum	53 pg/mL	[50]
	GCE	Multi-walled carbon nanotubes (MWCNTs)	Covalent (EDC/NHS)	Sandwich	AuNPs- 6-ferrocenyl hexanethiol	DPV	6-ferrocenyl hexanethiol	Spiked human serum	5.4 pg/mL	[51]
	GCE	Gold-Pd@SnO_2	Adsorption	Sandwich	Gold-mesoporous carbon nanocomposites-HRP-MB	DPV	MB	Spiked human serum	3.0 pg/mL	[52]
	Paper electrode	Gold nanorods (AuNRs)	Adsorption	Sandwich	Zinc oxide spheres-silver nanoparticles	Amperometry	H_2O_2	Patient serum	1.5 pg/mL	[53]
	GCE	Fc-modified hydrogel/CS/AuNPs	Adsorption	Label-free	n/a	SWV	Fc	Spiked human serum	0.5 pg/mL	[54]
	3D AuNW	Polypyrrole(Ppy)	Entrapment	Label-free	n/a	DPV	$[Fe(CN)_6]^{3-/4-}$	Spiked human serum	0.3 fg/mL	[55]
	GCE	MWCNTs/IL/CS/TH	Covalent (Phthaloyl chloride)	Sandwich	HRP	DPV	TH	Human serum	1.0 pg/mL	[56]
	ITO	Palladium NP-rGO	Covalent (EDC/NHS)	Label-free	n/a	Amperometry	$[Fe(CN)_6]^{3-/4-}$	Spiked human serum	10 pg/mL	[57]
	GCE	Graphene oxide (GO)	Covalent (EDC/NHS)	Sandwich	Fc-incorporated polystyrene spheres	SWV	Fc	Spiked human serum	1.0 pg/mL	[58]
	Vegetable parchment SPCE	Graphene	Covalent (GA)	Sandwich	AuNPs-HRP	LSV	H_2O_2	Patient serum	0.46 pg/mL	[59]
	AuE	MWCNTs/AuNPs	Adsorption	Sandwich	MWCNT-HRP	SWV	$[Fe(CN)_6]^{3-}$	Spiked human serum	0.40 pg/mL	[60]

Table 5. continued

Biomarker	Transducer	Surface modification	Immobilization	Assay	Label	Technique	Detection	Sample	LOD	Ref.
	GCE	Nafion/Cross-linked starch-MWCNTs/AuNP	Adsorption	Label-free	n/a	CV	$[Fe(CN)_6]^{3-/4-}$	Patient serum	7.0 pg/mL	[61]
	GCE	Graphene sheets – methylene blue – chitosan (GS-MB-CS)	Covalent (GA)	Label-free	n/a	Amperometry	MB	Patient serum	13 pg/mL	[62]
			Covalent (PBSE)	Sandwich	CdS quantum dots-GS	SWV	Cadmium	Patient serum	3.0 pg/mL	[63]
	GCE	GS/cobalt hexacyanoferrate NP	Covalent (PBSE)	Label-free	n/a	Amperometry	Cobalt hexacyanoferrate NP	Patient serum	10 pg/mL	[64]
	GCE	GS	Covalent (EDC/NHS)	Sandwich	Dopamine-Fe_3O_4–Fc-monocarboxylic acid	SWV	Fc monocarboxylic acid	Spiked serum	2.0 pg/mL	[65]
	GCE	Nanoporous Au	Adsorption	Label-free	n/a	CV	$[Fe(CN)_6]^{3-}$	Patient serum	3.0 pg/mL	[66]
	GCE	GS	Covalent (PBSE)	Sandwich	GS/TH/HRP	Amperometry	TH	Patient and spiked serum	1.0 pg/mL	[67]
	AuE	Cysteamine	Covalent (GA)	Sandwich	AP-encapsulated liposomes	LSV	Silver	Patient serum	7.0 pg/mL	[68]
	Dual-SPCE	AuNPs	Adsorption	Sandwich	AP	LSV	Silver	Human prostate tumour cell cultures	1.0 ng/mL	[69]

AuE: Gold electrode; AP: Alkaline phosphatase; CV: Cyclic voltammetry; DPV: Differential pulse voltammetry; EDC: 1-ethyl-3-(3-dimethylaminopropyl)-carbodiimide; Fc: ferrocene; GA: Glutaraldehyde; GCE: Glassy carbon electrode; H_2O_2: Hydrogen Peroxide; HRP: Horseradish peroxidise; LSV: linear sweep voltammetry; MB: Methylene blue; NHS: N-hydroxysuccinimide; PBSE: 1-pyrenebutanoic acid, succinimidyl ester; PSA: Prostate-Specific Antigen; SPCE: Screen-printed carbon electrode; SWV: Square wave voltammetry; TB: Toluidine blue; TH: Thionine; TMB: 3,3′,5,5′-Tetramethylbenzidine.

Table 6. Liver cancer biomarker analysis with electrochemical immunosensors.

Biomarker	Transducer	Surface modification	Immobilization	Assay	Label	Technique	Detection	Sample	LOD	Ref.
AFP	MGCE	Fe_3O_4-ε-Polylysine-heparin nanoparticles (Fe_3O_4-ε-PL-Hep)	Adsorption	Label-free	n/a	DPV	$[Fe(CN)_6]^{3-/4-}$	Human blood samples	0.072 ng/mL	[70]
	GCE	Heparin-polyglutamic-polypyrrole nanoparticles (Hep-PGA-PPy)	Covalent (EDC/NHS)	Label-free	n/a	DPV	$[Fe(CN)_6]^{3-/4-}$	Human blood samples	0.099 ng/mL	[71]
	GCE	CS–Au/Hyperbranched polyester nanoparticles-nitrite groups	Electrostatic interaction	Label-free	n/a	DPV	$[Fe(CN)_6]^{3-/4-}$	Spiked human serum	0.055 ng/mL	[72]
	GCE	Graphene oxide (GO)	Covalent (EDC/NHS)	Sandwich	Hydroxyapatite nanoparticles (HAPNPs)	SWV	Molybdate	Human serum	50 fg/mL	[73]
	GCE	Cuprous oxide nanowires decorated graphene oxide nanosheets-toluidine blue (Cu_2O@GO-TB)	Covalent (EDC/NHS)	Label-free	n/a	SWV	TB	Spiked human serum	0.1 fg/mL	[74]
	GCE	PANI/AuNPs/PEG	Covalent (EDC/NHS)	Label-free	n/a	DPV	PANI	Spiked serum samples	0.007 pg/mL	[75]
	GCE	Graphene/Gold nanoparticles (Gr/AuNP)	Adsorption	Sandwich	Poly(MB)-Au nanocomposites	SWV	MB	Patient serum	19.6 fg/mL	[76]
	GCE	N-doped multi-walled carbon nanotube (N-MWCNT)/Poly-dopamine (PDA)	Adsorption	Sandwich	GS/Au@Pt nanodendrites	Amperometry	H_2O_2	Spiked serum samples	0.05 pg/mL	[77]
	GCE	AuNPs	Adsorption	Sandwich	GS/ CeO_2 mesoporous nanopaticles (M–CeO_2)/ APTES/Pd octahedral nanoparticles (Pd)	Amperometry	H_2O_2	Spiked human serum	3.0 fg/mL	[78]
	GCE	Molybdenum carbide nanotubes / Thionine (Mo_2C/TH)	Covalent (GA)	Label-free	n/a	DPV	TH	Patient serum	3.0 pg/mL	[79]
	GCE	AuNPs	Adsorption	Sandwich	Biotin (B)-functionalized amination magnetic nanoparticle (APTES@Fe_3O_4)	Amperometry	H_2O_2	Spiked serum samples	0.33 pg/mL	[80]
	GCE	Carbon nanotubes/Gold nanorod (CNTs/Au NR)	Adsorption	Sandwich	HRP	DPV	TMB	Human serum	30 pg/mL	[81]
	GCE	β-Cyclodextrin – graphene (nano) sheets (β-CD-GS)	Covalent (EDC/NHS)	Sandwich	PdNi-NPs/N-doped Gra nanoribbons	Amperometry	H_2O	Human serum	0.03 pg/mL	[82]
	GCE	Gra/SnO_2/Au	Adsorption	Label-free	n/a	DPV	$[Ru(NH_3)_6]^{3+}$	Spiked serum samples	10 pg/mL	[83]
	Paper-based microfluidic devic	AuNW/GS	Adsorption	Sandwich	Copper sulfide/graphene oxide (CuS/GO)	Amperometry	H_2O_2	Patient serum	0.5 pg/mL	[84]
	GCE	AuNPs	Adsorption	Sandwich	Pb^{2+}@Au@MWCNTs-Fe_3O_4	Amperometry	H_2O_2	Serum samples	3.3 fg/mL	[85]

Table 6. continued

Biomarker	Transducer	Surface modification	Immobilization	Assay	Label	Technique	Detection	Sample	LOD	Ref.
	GCE	MWCNTs	Covalent (EDC/NHS)	Sandwich	Carbon decorated Fe_3O_4 magnetic microspheres @palladium (Fe_3O_4@C@Pd)	Amperometry	H_2O_2	Human serum	0.16 pg/mL	[86]
	GCE	AuNRs	Adsorption	Label-free	n/a	CV	$[Fe(CN)_6]^{3-/4-}$	Patient serum	40 pg/mL	[87]
	GCE	CD-GS	Adsorption	Sandwich	Pt@CuO-MWCNTs	Amperometry	$[Fe(CN)_6]^{3-/4-}$	Patient serum	0.33 pg/mL	[88]
	GCE	GS/copper oxide nanoflowers/AuNPs	Adsorption	Label-free	n/a	Amperometry	H_2O_2	Human serum	5.3 fg/mL	[89]
	3D AuE	3-mercaptopropionic acid (MPA)	Covalent (EDC/NHS)	Sandwich	HRP	Amperometry	TMB	Patient serum	3.0 pg/mL	[90]
	GCE	CS-AuNPs	Adsorption	Label-free	n/a	LSV	H_2O_2	Patient plasma	40 pg/mL	[91]
	GCE	Pd-rGO	Adsorption	Label-free	n/a	DPV	H_2O_2	Patient serum	5.0 pg/mL	[92]
	GCE	AuNPs/multifunctional mesoporous silica/toluidine blue (TB)	Adsorption	Sandwich	Au@MCM-41/TB	DPV	TB	Patient serum	0.05 pg/mL	[93]
	AuE	CS-SWCNTs/AuNPs	Affinity (Protein A)	Sandwich	Hollow AuNPs-HRP-TH	DPV	TH	Patient serum	8.3 pg/mL	[94]
	GCE	Pd nanoplates	Adsorption	Label-free	n/a	SWV	$[Fe(CN)_6]^{3-/4-}$	Patient serum	4.0 pg/mL	[95]
	GCE	rGO/Nafion/AuNPs	Adsorption	Sandwich	GOD-HPtNPs-Fe_3O_4-TH	DPV	TH	Human serum	1.6 pg/mL	[96]
	GCE	AuNPs/PDA/TH/GO	Adsorption	Label-free	n/a	DPV	TH	Human serum	30 pg/mL	[97]
	Pt	Poly (3,4-ethylenedioxythiophene) (PEDOT)/AuNPs/Azure I/ZnSe quantum dots	Adsorption	Label-free	n/a	CV	Azure I	Patient serum	1.1 fg/mL	[98]
	GCE	Polyamidoamine dendrimers/carbon dots/Au	Adsorption	Label-free	n/a	DPV	$[Fe(CN)_6]^{3-/4-}$	Patient serum	25 fg/mL	[99]

AFP: α-1-Fetoprotein; AuE: Gold electrode; GCE: Glassy carbon electrode; CV: Cyclic voltammetry; DPV: Differential pulse voltammetry; EDC: 1-ethyl-3-(3-dimethylaminopropyl)-carbodiimide; GA: Glutaraldehyde; GOD: Glucose oxidase; H_2O_2: Hydrogen Peroxide; HRP: Horseradish peroxidise; LSV: linear sweep voltammetry; MB: Methylene blue; MGCE: magnetic glassy carbon electrode; NHS: N-hydroxysuccinimide; PANI: Polyaniline; Pt: Platinum electrode; SWV: Square wave voltammetry; TB: Toluidine blue; TH: Thionine; TMB: 3,3′,5,5′-Tetramethylbenzidine.

Table 7. Stomach cancer biomarker analysis with electrochemical immunosensors.

Biomarker	Transducer	Surface modification	Immobilization	Assay	Label	Technique	Detection	Sample	LOD	Ref.
CA72-4	GCE	Nanoporous gold (NPG)	Adsorption	Sandwich	Polyaniline-Au asymmetric multi-component nanoparticles (PANi-AuAMNPs)	Amperometry	H_2O_2	Spiked serum samples	0.10 U/mL	[100]
	GCE	Reduced graphene oxide – tetraethylene pentamine (rGO-TEPA)	Covalent (EDC/NHS)	Sandwich	Dumbbell-like PtPd-Fe_3O_4 NPs	Amperometry	H_2O_2	Patient serum	0.3 mU/mL	[101]
IL-6	GCE	3-3'-Dithio-bis (propionic acid NHS)/Ferrocenyltethered dendrimer/AuNP	Adsorption	Sandwich	HRP	Amperometry	Ferrocenyl-tethered dendrimer	Patient serum	1.0 pg/mL	[102]

CA 72-4: Cancer Antigen 72-4; EDC: 1-ethyl-3-(3-dimethylaminopropyl)-carbodiimide; GCE: Glassy carbon electrode; HRP: Horseradish peroxidise; H_2O_2: Hydrogen Peroxide; IL-6: Interleukin-6; NHS: N-hydroxysuccinimide.

negatively charged ligand. Briefly, the synthesis involves a solution containing $HAuCl_4$ and ultrapure water that is refluxed at high temperature. Then, under magnetic stirring, the reducing agent sodium citrate is added. After adequate cooling of the solution, a drop of the obtained AuNPs was placed on the working electrode and allowed to disperse. Anti-PSA antibodies were immobilized by physical and chemical binding. Besides AuNPs, other subtypes of gold nanomaterials were also reported to improve the sensor performance: gold nanorods (AuNRs) [53,87] and nanoporous gold (NPG), that can also be used to efficiently immobilize the bioreceptor element. Wei et al. [66] prepared a NPG film with uniform pore size and large surface area by a dealloying method, which allowed the adsorption of the antibody into the pores of the film and provided a low detection limit.

On the other hand, carbon-based nanomaterials are also used in transducer surface modifications because of several reasons: (i) the increase of the surface area and subsequent increase of sensitivity; (ii) immobilization of a large amount of biomolecules, and (iii) their unique characteristics and properties, especially their excellent electrical conductivity [108]. Distinct dimensional carbon-based nanomaterials can be used, such as carbon nanotubes (CNTs) that contemplate single-walled carbon nanotubes (SWCNTs) [17] and multi-walled carbon nanotubes (MWCNTs) [51,86] or graphene (Gra) which contemplates graphene (nano) sheets (GS) [59,65,67], nitrogen-doped graphene sheets (N-GS) [20,22,35], graphene oxide (GO) [33,58] and reduced graphene oxide (rGO) [21,101]. Recent progress in the synthesis of graphene-based hybrid nanomaterials have made them even more appreciated, benefiting from the electrochemical catalytic properties and the higher electron transfer rate between the electrode and the detection molecules [15,109]. For example, Zhang et al. [15] reported a sandwich-type immunoassay using carbon nanosphere-functionalized graphene hybrid nanosheets on a glassy carbon electrode (GCE) as sensing platform. The use of functionalized graphene nanosheets increases the surface area for the immobilization of biomolecules.

Furthermore, the conjugation between gold- and carbon-based nanomaterials and/or ionic liquids offer multiple options in the sensor's construction. Improved performances were achieved using distinct combinations, such as AuNC/nickel hexacyanoferrate NPs/AuNP-GS [18], MWCNTs/AuNPs [24,60], AuNPs/Fc-rGO [34], AuNPs-porous GO [41], MWCNTs/gold colloids [43], Nafion/MWCNTs/AuNPs [61], AuNRs/CNTs [81], gold nanowires (AuNW)/GS [84], chitosan (CS)-SWCNTs/AuNPs [94], rGO/nafion/AuNPs [96], AuNPs/PDA/TH/GO [97].

For example, Yang et al. [41] reported a sensing platform composed of AuNPs functionalized porous graphene (Au-PGO). In this sandwich-type electrochemical immunosensor for the determination of CA 19-9, an Au-PGO nanohybrid structure provided a large accessible surface area for the immobilization of the antibodies,

which also facilitated electron transfer, leading to a further enhancement of the sensor's sensitivity. In addition, Li et al. [84] reported an immunosensor for the detection of AFP using a hybrid nanostructure for effective antibody immobilization. The sensing platform was prepared by in situ solution-phase synthesis using non-covalent ultrathin gold nanowires (AuNWs) functionalized graphene sheets (GS). The water-soluble AuNWs/GS hybrid allowed efficient electrochemical sensing and combined the advantages of the carbon- and gold- based nanomaterials. The developed sensor was successfully applied to the analysis of serum samples from both healthy individuals and cancer patients.

Besides gold and carbon, other nanomaterials have also been used to easily conjugate nano- and biomaterials and biomolecules in the construction of disposable and sensitive immunosensors and immunoassays. Hong et al. [38] developed an electrochemical immunosensor for the detection of CA 15-3 using ferrocenecarboxylic acid (Fc-COOH)-doped silica nanoparticles (SNPs) as an affinity support on a AuE. The use of colloidal silica prevented the leakage of Fc-COOH which was easily modified with a trialkoxysilane. The NH_2 groups on the nanoparticles' surfaces allowed the covalent immobilization of CA 15-3 antibodies using glutaraldehyde as crosslinking agent. In another work, Yang et al. [52] electrodeposited AuNPs onto the surface of a Pd@flower-like SnO_2 nanocomposite for effective antibody immobilization, leading to an enhancement of the sensitivity of the immunosensor. In another approach, Li et al. [64] developed a label-free immunosensor for PSA detection based on the binding of the antibody to a thin film composed of graphene sheet (GS) and cobalt hexacyanoferrate nanoparticles (CoNP) on a GCE. The synergistic effect between the nanomaterials was investigated and showed that the electroactivity of CoNP was greatly improved in the presence of GS and that the formed composite film displayed high electroactivity and good stability.

Based on the unique characteristics of an graphene/SnO_2/Au nanocomposite, an immunosensor for AFP detection was developed through layer-by-layer self-assembly on a GCE [83]. The good biocompatibility of the nanocomposite provided suitable conditions for the interaction between antibody and antigen and the combination of graphene, SnO_2 and Au provided the efficient detection of the biomarker.

Xu et al. [71] reported an immunosensor that could be applied to the analysis of AFP in whole blood samples by using heparin-polyglutamic-polypyrrole (Hep-PGA-PPy) nanoparticles. The construction of the sensor was based on the immobilization of anti-AFP antibodies on the Hep-PGA-PPy nanoparticles that were then dropped on a GCE surface (previously modified with APTES) and fixed on the sensing surface through electrostatic bonding. The Hep-PGA-PPy nanoparticles improved the anti-biofouling effect of the electrode by combining the distinct characteristics of the nanoparticle components. The developed immunosensor exhibited a low limit of detection (0.099 ng/mL).

Biomaterials have also been introduced in the surface modification strategy and are often coated with nanomaterials to improve the performance of the biosensor [54,62,91,99]. An interesting work developed by Gao et al. [99] was based on polyamidoamine dendrimers capped-carbon dots (PAMAM-CDs)/Au nanocrystal nanocomposites as an immobilization matrix on a GCE for sensitive immunosensing of AFP. The referred matrix offered the possibility to combine distinct nanomaterials to form nanocomposites, which exhibited excellent conductivity, stability and biocompatibility of the electrode's surface.

6 Antibody Immobilization

For the development of immunosensors, as for the majority of biosensors, the immobilization of the antibody on the sensor‘s surface is crucial to achieve adequate performance characteristics (e.g. high sensitivity and precision, short response times, etc.) and long-term stability. It is therefore important to minimize antibody denaturation and conformational changes during or after immobilization [110]. The orientation of the antibodies and the low non-specific adsorption on the sensing surface are critical factors for the effective detection of the antigen. In general, the antibodies' functional groups are allowed to react and bind with the functional groups available on the distinct (modified) sensing platforms. Thus, for the development of electrochemical immunosensors several antibody immobilization strategies have been explored, including: non-covalent (adsorption and entrapment), covalent and affinity approaches.

The adsorption strategy is the most easily performed and consists of casting an antibody solution on the electrode's surface or dipping the electrode in an antibody solution. Then, after an appropriate incubation time, the electrode is washed to remove non-adsorbed antibodies. The major drawbacks of this technique are the random orientation of the antibodies, which exhibit lower antigen binding capacities than properly orientated antibodies [110], and the formation of weak bonds between the antibody and the transducer, which can lead to the loss of antibody during analysis and storage. In the adsorption process, the interaction between the antibodies and the electrode surface can be classified as electrostatic or hydrophobic. In this strategy, distinct carbon- and gold-based nanomaterials are typically used as platforms for the efficient binding of antibodies. The interaction between antibodies and gold nanomaterials (mainly AuNPs) are usually achieved by chemisorption via thiol derivatives, involving a chemical adsorption process between the nanomaterial surface and the adsorbent surface, which causes the bond to be created [14,25,27,48,69,78,80,85,87]. As an example, Wang et al. [14] described the immobilization of antibodies through adsorption onto AuNPs electrodeposited on a hydrogel film, that

was used as an electrochemical immunosensing substrate for the detection of NSE in serum samples.

Another type of non-covalent immobilization is entrapment. In this process, the biological recognition element can be immobilized within a suitable matrix. Normally, the biocomponent is mixed with the supporting (nano) material and then deposited on the electrode surface. Electropolymerization is also often used for biomolecule entrapment. Moon et al. [55], suggested a label-free immunosensor for PSA by incorporating the anti-PSA antibody into polypyrrole. The electropolymerization of polypyrrole on an Au nanowire array was the key strategy in this study where anti-PSA antibodies could simultaneously be immobilized on individual polypyrrole nanowires, without additional modification steps, resulting in enhanced molecular interactions. The nanowires served as an efficient reservoir for the incorporation of high concentrations of anti-PSA antibodies. Indeed, the large surface area and well-defined nanowire structure make them ideal for efficient antibody immobilization and thus, to enhance the loading capacity. In addition, the preferential electrostatic association between positive charges of the oxidized polypyrrole chains and negative carboxyl groups on the antibody allows strong immobilization while ensuring antigenic epitope conservation.

Very stable linkage of the antibody to the sensor surface can be achieved through covalent binding between functional groups present on the (chemically modified) transducer surface and the antibody. Nevertheless, care must be taken not to bind functional groups essential for antigen binding. Examples of compounds used for this purpose are the well-known combination of 1-ethyl-3-(3-dimethylaminopropyl)-carbodiimide and N-hydroxysuccinimide (EDC/NHS). Glutaraldehyde (GA), 1-pyrenebutanoic acid succinimidyl ester (PBSE), phthaloyl chloride and iminithiolane can also be used. Many immunosensors were described in which carbodiimide chemistry was employed for antibody immobilization [17,26,31,32, 35,51,57,58,65, 82,86,90,101]. In general, in this process the primary amine groups of the antibody are covalently bound to the carboxylic acid group present on the sensor surface, through reactive succinimide esters by amine coupling through EDC/NHS chemistry. On the other hand, aldehyde modification is a suitable strategy to use when the sensor's surface is functionalized with materials containing chemical groups such as amines or alcohols to form imines. Basically, the modified sensing surface is treated with glutaraldehyde (or other aldehydes) that is allowed to react with the antibodies' functional groups. Like this, the binding between the surface and the biological compound is accomplished through the cross-linking agent [20–22,36,38,40, 46,50,59,68,79].

Antibodies can also be covalently immobilized onto the working electrode through PBSE, based on an amidation reaction between the available amine groups of the antibody and the succinimidyl ester group of PBSE [64,67]. Yang et al. [67] developed an immunosensor for prostate cancer biomarker detection by immobilization of the primary antibody onto the surfaces of GS through PBSE which was adsorbed onto the nanomaterial through π–π stacking.

In addition, self-assembly provides a convenient and simple way of creating a highly ordered thin molecular film with tailored chemical properties. In this process, the thin molecular layer is formed by adsorption of molecules from solution onto a solid surface. Subsequently, the adsorbates spontaneously arrange themselves until a completely ordered molecular monolayer is formed, which is called the self-assembled monolayer (SAM) [111], and onto which antibodies can be immobilized. Qu et al. [68] used cysteamine to produce a SAM on the sensor platform and covalently bound the capture antibody through glutaraldehyde. Emami et al. [28] proposed the construction of a label-free immunosensor composed of distinct layers for HER2 detection. Firstly, AuNPs were electrodeposited on a gold electrode surface, followed by the immersion of the electrode in a 3-mercaptopropionic acid (MPA) solution to form the SAM. Then, ECD/NHS was added to activate the carboxyl groups of the MPA layer. Subsequently, cysteamine was added and bound via amide formation. Thereafter, pegylated magnetic iron nanoparticles bound to the thiolated antibodies were added to the previously formed layer-by-layer sensing surface.

Affinity as an immobilization process consists of the interaction between intermediate binding biomolecules (e.g. Protein A, Protein G, biotin, avidin or streptavidin) or carbohydrates (β-cyclodextrin) and a part of an antibody, known as the Fc region. These non-covalent interactions are usually very strong and are adequate to preferentially orient the antibodies and immobilize them successfully on the electrode platform.

Li et al. [94] reported a multi-step sensor platform approach by casting SWCNTs dispersed in chitosan (CSSH-SWCNTs) on the electrode. This process allowed the formation of a multitude of thiol groups (–SH) onto which AuNPs were immobilized. Subsequently the electrode was incubated with protein A (PA) which provided adequate orientation of antibodies on the electrode surface. Park et al. [33] compared the biosensing performance of electroreduction-based electrochemical-enzymatic redox-cycling schemes for the detection of cancer antigen CA 15-3 by using avidin in the surface modification. In this sensor, biotinylated anti-CA-15-3 IgG antibodies were placed on avidin-modified ITO electrodes for adequate orientation (Figure 1), and a detection limit of 0.100 U/mL was obtained.

7 Assay Formats (Immunochemical Interactions)

In EI, the most common immunochemical (antibody-antigen) assay formats are: non-competitive (sandwich), label-free and competitive assays, which are schematized in Figure 2.

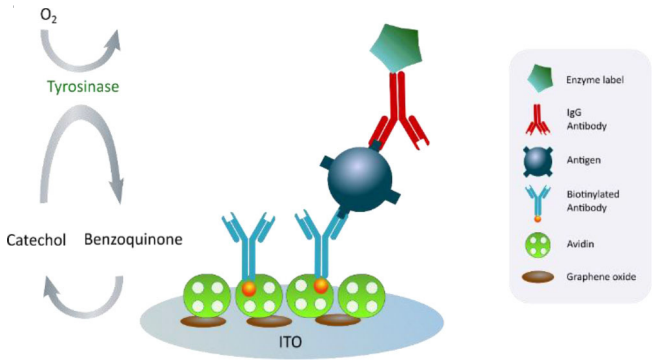

Fig. 1. Schematic Representation of an Electrochemical Immunosensor based on GO and Avidin modified sensing platform [33]. Re-drawn using Inkscape software.

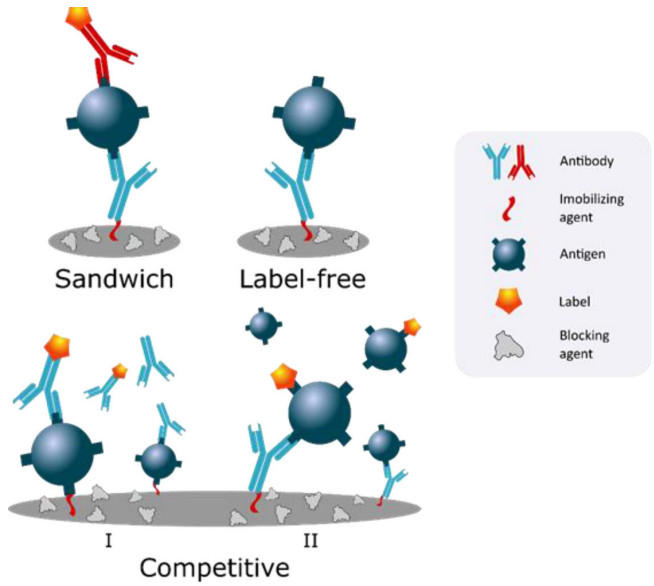

Fig. 2. Types of immunoassays (I – immobilized antibodies react with free antigens in competition with labelled antigens, II – immobilized antigens react with free and labelled antibodies.

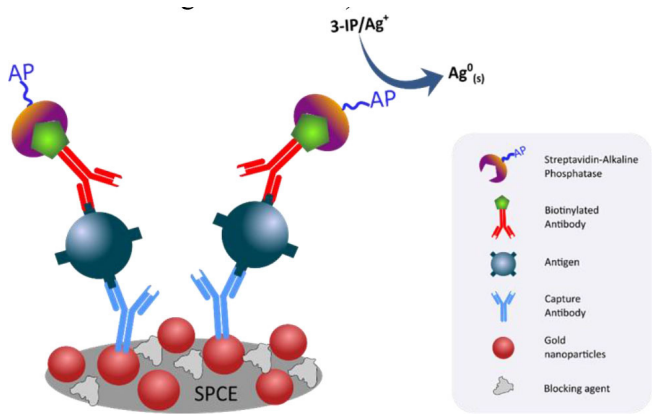

Fig. 3. Schematic representation of a sandwich immunosensor for breast cancer protein biomarker detection [27]. Re-drawn using Inkscape software.

In the non-competitive (sandwich) assay, a capture antibody is immobilized on the electrode‘s surface which is subsequently blocked using an inert protein (e. g. BSA or casein) to avoid non-specific adsorption. The sensor is then incubated with the sample, and the antigen (cancer biomarker) is bound to the antibody‘s binding site. Then a secondary antibody is added to complete the sandwich format. In this type of assays the secondary antibody is usually labelled to enable the detection of the antibody-antigen interaction and/or to enhance the analytical signal [27]. Enzymes such as alkaline phosphatase (AP), horseradish peroxidase (HRP) are classic examples of such labels. When enzymatic labels are used, the enzymatic substrate is placed on the sensor’s surface after the incubation with the secondary antibody and one of the enzymatic reaction products can be monitored. In this case, the electrochemical signal is proportional to the concentration of the electroactive product which in turn is proportional to the amount of enzymatic label and subsequently to the concentration of the antigen in the sample. The use of enzyme labels provides significant signal amplification, resulting in extremely low detection limits [112]. In EI for the analysis of cancer biomarkers, the most frequently used enzymes are AP and HRP. Examples of immunosensors in which the AP label was used are: Marques et al. [27] for the detection of HER2 and Escamilla-Gomez et al. [69] for the detection of PSA. In these works, the antibody-antigen interaction was measured by using a combination of 3-indoxyl phosphate (3-IP), an enzymatic substrate of AP, and silver ions (Figure 3), leading to the formation of metallic silver which was detected by LSV. The use of silver ions increases the electrochemical signal when compared to the use of 3-IP alone, allowing detection limits below the cut-off values for the mentioned biomarkers (4.4 ng/mL for HER2 and 1.0 ng/mL for PSA).

In another approach, the use of liposomes, as carriers of the marker molecules, can also amplify the signal and improve the sensitivity of the immunosensor. A similar sandwich assay developed by Escamilla-Gomez et al. [69] for PSA detection was performed by Qu et al. [68]. However, in the latter study, AP was encapsulated in liposomes. After the immunological interactions, the bound liposomes were lysed with Triton X-100 to release the encapsulated AP, which converted ascorbic acid 2-phosphate (AA-p) into ascorbic acid and, in the presence of silver ions, led to deposition of the metallic silver.

Besides the use of AP, HRP is used in a wide range of sensor approaches. In the sensor developed by Mucelli et al. [30], secondary antibodies labelled with HRP and methylene blue (MB) were used to detect the interaction between the protein and the antibody. MB is extensively employed as mediator or electrochemically active agent in cancer biosensors. Here, the electrochemical signal is generated by MB (added as soluble mediator) which shuttles electrons from the electrode to HRP during the enzymatic reaction with its substrate, H2O2. In addition, Biscay et al. [49], Guo et al. [81] and Zhong et al. [90]

used similar methodologies based on HRP as label and 3,3′,5,5′ tetramethylbenzidine (TMB) as co-substrate. The authors combined TMB and H_2O_2 to apply a less positive potential and thus avoid some interferences.

Enzymes can also be combined with metallic (nano) materials and/or with redox mediators to obtain more efficient electrochemical signal amplifications. In the work developed by Li et al. [94] a sandwich-type electrochemical immunoassay was constructed based on an efficient signal amplification strategy using hollow AuNPs, HRP NP bioconjugates and TH. Here, TH was used as mediator between HRP enzyme and the electrode surface, and then HRP could synergistically catalyse H_2O_2. TH is highly redox active and improves the intensity of the signal (Figure 4).

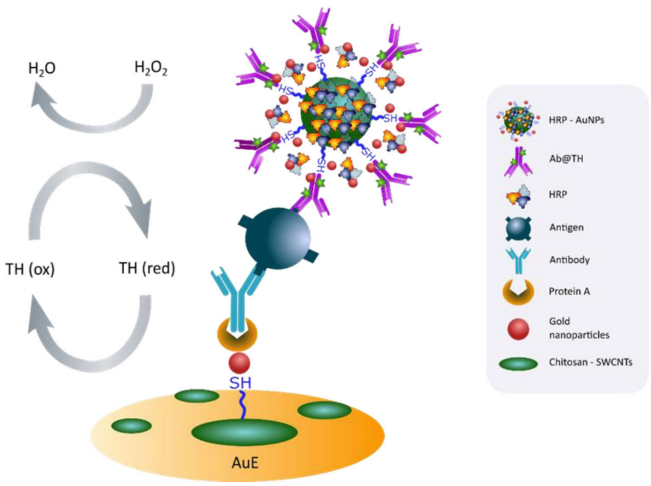

Fig. 4. Electrochemical signal amplification strategy [94]. Redrawn using Inkscape software.

However, the drawbacks of loaded enzymes limit their use as labels in electrochemical immunosensors because of: (i) easy inactivation; (ii) costly preparation; (iii) laborious purification processes. Therefore, nanomaterials with electrocatalytic properties for the electrochemical detection of H_2O_2 are frequently employed to: (i) enhance the sensitivity achieved in the analysis, (ii) reduce the detection potential to minimize the interference of other species present in the sample. A disadvantage of H_2O_2 detection is the high detection potential, which can also lead to the oxidation of other substances present in the sample.

Jiang et al. [80] developed an amplification option for a sandwich-type immunosensor based on biotin-functionalized amination of a magnetic nanoparticle composite (B-APTES@Fe_3O_4) as label for detection of AFP. The strategy was successfully implemented using a biotin-streptavidin-biotin (B-SA-B) network. Here, further signal amplification could be achieved as SA and BAPTES@Fe_3O_4 are added layer by layer on the electrode. In addition, B-APTES@Fe_3O_4 was used as label of the secondary antibody, which catalysed the electrochemical reaction of H_2O_2.

In the immunosensor for PSA detection developed by Chu et al. [48], Pd@Cu_2O NPs were used as label and presented the excellent characteristics of palladium- (Pd NPs) and cuprous oxide nanoparticles (Cu_2O NPs).

An enzyme-free immunosensor for PSA detection was constructed by Sun et al. [53], using porous zinc oxide spheres-silver nanoparticles (ZnO_2–AgNPs) nanocomposites as signal labels. The large surface area of ZnO_2 provided sites for the inclusion of AgNPs which improved their catalytic capacity toward H_2O_2 reduction. This allowed the construction of enzyme-free electrochemical sensors which are cheaper and simpler than enzyme-labelled immunosensors.

Moreover, metal ions and quantum dots (QDs) seem to be promising candidates as labels. Commercially available QDs are normally preferred because their preparation is complicated and tedious. However, the drawbacks of using QDs include the rather harsh conditions needed to dissolve QDs and the need for a highly sensitive stripping technique to obtain the signal [32]. Distinct sensing strategies for metal ions/QD-based biosensors can be performed by using several ions (e.g. Cd^{2+}, Pb^{2+}, Cu^{2+}, Zn^{2+}) for direct labelling, avoiding the above-mentioned problems. Zhao et al. developed an immunosensor for detection of the breast cancer biomarker CA 15-3 where Cd^{2+}-functionalized nanoporous TiO_2 (TiO_2–Cd^{2+}) was used as label for the detection of the signal [32]. Nanoporous TiO_2 spheres were used because of its highly specific surface area (functionalized with abundant $–NH_2$ groups) which are favourable for the adsorption of high amount of Cd^{2+} which was subsequently detected by SWV, allowing to obtain a detection limit of 0.008 U/mL.

In the label-free approach the antibody-antigen interaction is detected directly without the need of a secondary antibody. This simplifies the immunoassay, allowing faster and cheaper analysis [113]. In these assays, like in the sandwich technique, an antibody is immobilized on the transducer's surface and the immunocomplex is formed after incubation with a sample. Then a redox probe is placed on the sensor and the analytical signal is recorded. The amplitude of this signal decreases with increasing antigen concentration because of the electron transfer hindrance caused by the formed immunocomplex. The most commonly employed redox probes in the label-free approach for cancer immunosensors are: $[Fe(CN)_6]^{3-/4-}$ [18,24,25,28,35, 46, 50,55,57,61,66,87,95,99], Prussian blue (PB) [19,39], Ferrocene (Fc) [34,54], Ferrocenecarboxylic acid (Fc-COOH) [38], Methylene Blue (MB) [62], Cobalt hexacyanoferrate NPs [64], thionine (TH) [79,97], $[Ru(NH_3)_6]^{3+}$ [83], H_2O_2 [89,91,92], Azure I [98]. As an example, the $[Fe(CN)_6]^{3-/4-}$ redox probe was used by Deng et al. [46] in a label-free immunoassay for trace species analysis, based on the "gate-effect" of a β-cyclodextrin (β-CD) layer. In this work, the detection of PSA was carried out using a β-CD assembled layer, which created gates for

the electron transfer of the probe. The monoclonal antibody labelled β-CD and the interspaces between β-CD molecules in the layer were formed on the electrode, which act as a channel for the electron transfer from the probe (Figure 5). By virtue of the "gate-effect", signal amplification and enhancement of the signal-to-noise ratio was achieved.

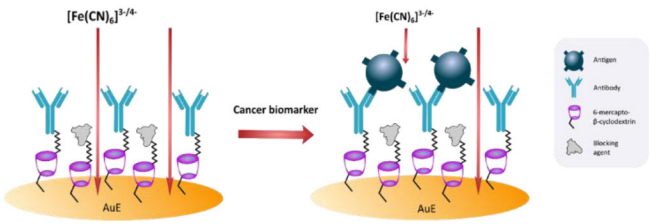

Fig. 5. Example of a label free assay, using $[Fe(CN)_6]^{3-/4-}$ as redox probe [46]. Re-drawn using Inkscape software.

Moreover, Mao et al. [62] used Methylene Blue (MB) as the redox probe in a label-free EI based on a nanocomposite film composed of graphene sheets-methylene blue-chitosan (GS-MB-CS). The film was used as electrode material to immobilize the antibody because of the high nanocomposite film binding affinity to the electrode. Another example of a redox probe is $[Ru(NH_3)_6]^{3+}$ that was used in a label-free immunosensor for the detection of AFP by monitoring the peak current change [83]. In this work, a graphene/SnO_2/Au nanocomposite sensor platform was used to immobilize the capture antibody. A decrease in the peak current intensity of $[Ru(NH_3)_6]^{3+}$ was related to the interaction between antibody and antigen.

Another assay type with a reduced number of applications in electrochemical immunosensing of cancer biomarkers is the competitive immunoassay. In this assay

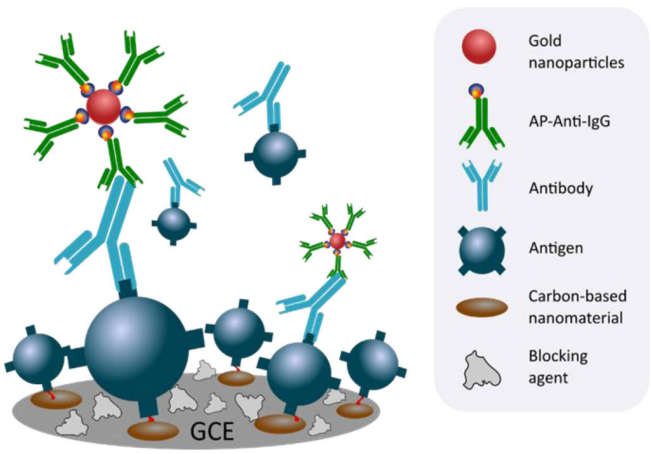

Fig. 6. Schematic representation of Competitive electrochemical immunosensor for NSE detection [17]. Re-drawn using Inkscape software.

(i) immobilized antibodies react with free antigens in competition with labelled antigens or (ii) immobilized antigens react with free and labelled antibodies [114]. The labels employed are identical to the ones used in non-competitive assays. Yu et al. [17] developed a competitive electrochemical immunosensor for the detection of NSE in serum. In the sensing phase construction, a drop of SWCNTs was cast onto a GCE electrode and EDC/NHS was added to activate the carboxyl groups, allowing efficient NSE binding. In this competitive format, the high loading of NSE on SWCNTs greatly extended the limit of the detectable range. For the competitive immunoreaction, the sensor was incubated with the sample (containing 'free' NSE) and anti-NSE antibodies. For the signal readout, AP-anti-IgG/AuNP was used, that exhibited high catalytic activity toward the hydrolysis of α-NP in DEA buffer (Figure 6).

8 Magnetic Immunoassays

In addition to the previously mentioned sensor surface modification based on nanomaterials and biomaterials, magnetic beads (MBs) are powerful tools for bioassays because of, for example, the increase of the surface area and the improvement of the sensitivity of the detection method [115]. Their use, combined with modified electrode surfaces improves biomolecule interactions and reduces or/and minimizes the matrix effect of the sample by efficient washing steps [116]. MBs can be manipulated with an external magnet that enables biological reaction events to be performed away from the electrode and can be retained on a sensor surface by an external magnetic field through, for example, the placement of small magnets below the surface of the working electrode (normally with the corresponding size of the WE). Therefore, the recognition element is not in direct contact with the electrode surface, which constitutes the major drawback related to the use of MBs [117]. MBs can be functionalized with distinct recognition elements generally through (i) affinity agents (e.g. Protein A, streptavidin) and (ii) covalent binding (e.g. EDC/NHS, GA, SAMs) (Figure 7).

Ilkhani et al. [23] reported three simple magnetic bead-based approaches, combined with screen-printed arrays, for the analysis of HER2. The bioassays were based on a sandwich format in which affibody (Af) or antibody molecules were immobilized on streptavidin- or protein A-modified MBs (Strept-MBs or Prot A-MBs). Both types of MBs could be used for immuno-precipitation purposes.

Al-Khafaji et al. [29] reported a magnetic immunoassay for HER2 detection by using protein A-modified magnetic beads. The proposed assay was based on a sandwich format in which antibody-functionalised magnetic beads were used to capture the protein biomarker. Then, anti-HER2 antibodies labelled with AP were added to trace the affinity reaction, using 1-naphthyl-phosphate as enzymatic substrate and DPV for signal detection.

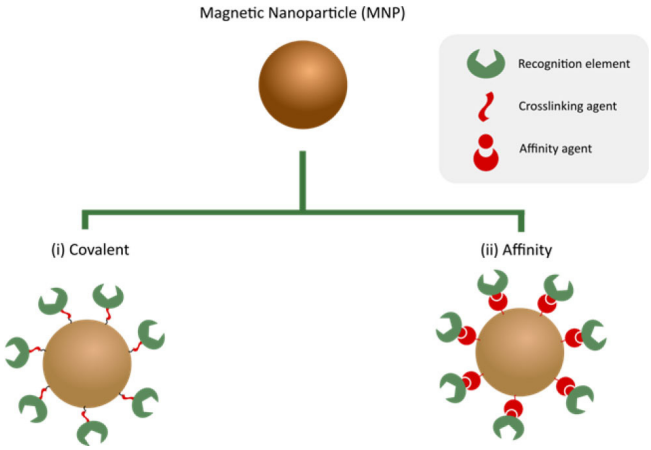

Fig. 7. Strategies on immobilization of recognition element onto the surface of magnetic particles.

Biscay et al. [49] investigated a screening device using magnetic beads as solid phase to develop an immunoassay for the detection of total PSA (tPSA) in serum. Here, the tPSA detection was performed by using superparamagnetic beads (1 mm) modified with streptavidin and an 8-channel screen printed electrode array. In this assay, a mixture of biotinylated antibodies and HRP-labelled antibodies were added to a previously prepared solution containing Strep-MBs and PSA, forming a sandwich complex. Then, TMB was added, which was subsequently oxidized in the reaction cascade and detected by chronoamperometry.

9 Simultaneous/Multiplex Detection

Screening and early diagnosis of cancer contributes to prognosis judgement and appropriate treatment of the patient. In clinical practice, the determination of a single specific biomarker is facing a great challenge and has limitations because of the poor specificity and sensitivity

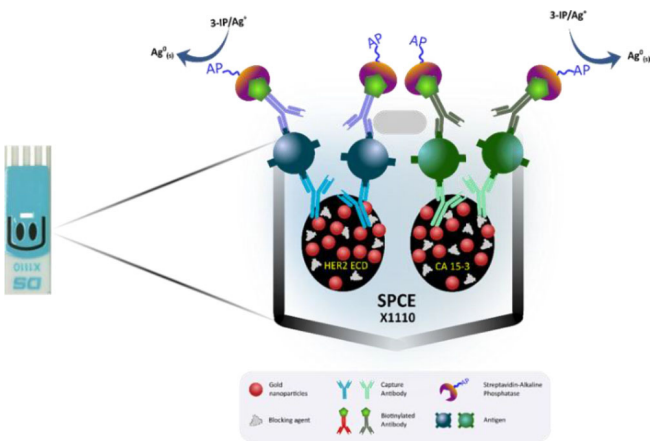

Fig. 8. Schematic representation of multiplexed detection of cancer biomarkers [118]. Re-drawn using Inkscape software.

between the tumour biomarker and the cancer type. Thus, simultaneous detection of multiple biomarkers is of utmost importance and may confer high diagnostic specificity of the disease. To address this, the design of (bio) sensors for the simultaneous detection of multiple tumour biomarkers has demonstrated significant improvements.

Multiplexed electrochemical immunoassays and/or immunosensors are feasible options to detect, identify and quantify two or more biomarkers in the same sample. A major issue in the development of these assays is related to the distinction between the signals of the multiple antigen–antibody interactions. One option is to use multi-working electrode sensors in which each WE is modified with a specific capture antibody. Another option is the use of antibodies with distinct labels (multi-labelling). In this last approach, the electrochemical detection based can be performed on single WE sensors.

Escamilla-Gomez et al. [69] reported the use of SPCEs that contain two carbon working electrodes for the simultaneous determination of prostate specific antigen (free PSA and total PSA). In this sensor, 8A6 anti-PSA and 5G6 anti-PSA antibodies were separately immobilized, through adsorption, on each of the WEs. Then, biotinylated antibodies and an S-AP conjugate were added, and the detection was accomplished using a substrate solution containing 3-IP and silver ions. The analytical signal was obtained by LSV and the results showed the feasibility of the simultaneous detection of fPSA and tPSA in human prostate tumour cells.

A similar approach with multi WE sensors was reported by Marques et al. [118]. In their strategy, a multiplexed electrochemical immunosensor for the simultaneous detection of two breast cancer biomarkers (CA 15-3 and HER2-ECD) was developed based on a customized dual screen-printed carbon electrode (bi-SPCE) nanostructured with in situ generated gold nanoparticles. The application of this bi-immunosensor was based on the antigen-antibody interactions, in which specific capture antibodies for these biomarkers were immobilized by adsorption on each nanostructured working electrode, and the electrochemical signals were detected by LSV analysis of enzymatically (AP) generated metallic silver (Figure 8). The immunosensor's limits of detection were 5.0 U/mL for CA 15-3 and 2.9 ng/mL for HER2-ECD.

10 Cytosensors

One of the major current challenges in cancer diagnostics and follow-up is the analysis of circulating tumour cells (CTCs). CTCs are cells that are shed from a primary tumour and circulate in the body. They contain a large amount of information on the tumour phenotype [119]. Due to the important information that can be obtained from CTCs, several detection methodologies have been developed that contribute to a more efficient diagnosis.

Therefore, cytosensors have emerged as an innovating area related to electrochemical (bio) sensors. Cytosensors

are a class of biosensors that can detect specific cells through their recognition by, for example, antibodies, aptamers, DNA, that are immobilized on a transducer surface. Although the analysis of CTCs is important in diagnosis, no analytical devices are currently available that allow their effective detection with low costs, small sample volumes and in situ detection.

CTCs originating from epithelial tumours express the epithelial cell adhesion molecule EpCAM [119–121]. Recently, cytosensors for CTCs detection using EpCAM have been described [122,123]. Shen et al. [122] developed a reusable cytocensor with self-assembled monolayers deposited onto an AuE to directionally insert the capture probe (EpCAM aptamer) which specifically binds to EpCAM over-expressed on the membrane of breast cancer MCF-7 cells. The electrochemical response of this label-free cytosensor towards MCF7 cells was recorded by EIS using the redox probe $[Fe(CN)_6]^{3-/4-}$. Maltez-da Costa et al. [123] developed a strategy for a simple monitoring and rapid electrochemical biosensing for CTCs quantification using specific antibodies labelled with magnetic beads (MBs). Human colon adenocarcinoma cell line (Caco2) was chosen as a model CTC because, similarly to other adenocarcinomas, Caco2 have a strong expression of EpCAM. In this cytosensor, the authors combined anti-EpCAM antibody-functionalized MBs with antibody-modified AuNPs in liquid suspensions. The detection of the labelled Caco2 cells was performed by chronoamperometry through the hydrogen evolution reaction, using 1 M HCl, that was electrocatalyzed by the AuNP labels. In another work, HER2-overexpressing cells could be detected using a hydrazine-AuNP-aptamer bioconjugate [124]. The developed sensor could differentiate between HER2-positive and HER2-negative breast cancer cells and could be applied to diagnosis through either HER2 protein or SK-BR-3 breast cancer cell in human serum samples. In the detection process the sensor was placed in a silver nitrate solution where silver ions were selectively reduced to metallic silver by hydrazine which was then oxidized using square wave stripping voltammetry (SWSV). Lu et al. [125] developed an electrochemical cytosensor for lung cancer cell detection that could sensitively differentiate A549 cells from normal ones (AT II cells) using an epidermal growth factor (EGFR) antibody to recognize EGFR receptors that are over-expressed on the cancer cells. To avoid the drawbacks related to the use of extra immobilization agents and enzymes, AuNPs decorated m-aminophenol based resin microspheres were used to act as suitable immobilization carriers and to facilitate electron transfer. The detection strategy used in this approach was based on the electron transfer blockage of the immunocaptured A549 cells.

11 Conclusions

The continuous progress and the evolution of analytical methodologies allow an increasingly effective diagnosis and follow-up of cancer. In this review, a short summary of recently developed voltammetric and amperometric immunoassays and cytosensors for the analysis of the six most commonly diagnosed cancer biomarkers is presented. A survey of the published studies shows that the attention in this research area is now mainly focussed on the increase of the sensitivity through different types of electrode surface modifications (carbon- and gold- based nanomaterials, nanoparticles, nanocomposites, SAMs and/or biomaterials) and detection labels of (secondary) antibodies. Magnetic immunoassays also constitute an adequate strategy because of the inherent advantages of using magnetic particles, since they enhance the interactions of the biomolecules and minimize the effect of the sample matrix. Moreover, the development of sensors that provide simultaneous or multiplexed detection contributes to a better prognosis and more efficient screening. The development of cytosensors is currently a challenge to improve cancer detection.

The low limits of detection attained with the developed sensors allows the detection of cancers in an early stage, which could prevent the deaths of millions of people and reduce the suffering of patients and their families and the cost to society. Furthermore, their high sensitivity enables the detection of only slight changes in the biomarker concentration. This could be an excellent additional tool for monitoring cancer patients during treatment and follow-up.

Acknowledgements

Maria Freitas is grateful to FCT-Fundação para a Ciência e a Tecnologia for her PhD grant (SFRH/BD/111942/2015), financed by POPH-QREN-Tipologia 4.1-Formação Avançada, subsidized by Fundo Social Europeu and Ministério da Ciência, Tecnologia e Ensino Superior. This work received financial support from the European Union (FEDER funds through COMPETE) and National Funds (FCT) through project UID/QUI/50006/2013.

References

[1] J. Ferlay, I. Soerjomataram, R. Dikshit, S. Eser, C. Mathers, M. Rebelo, D. M. Parkin, D. Forman, F. Bray, *Int. J. Cancer.* **2014**, *136*, E359–E386. Available from: http://globocan.iarc.fr.

[2] WHO. Cancer, Fact sheet N°297. Available from: http://www.who.int/mediacentre/factsheets/fs297/en/#.

[3] C. Paoletti, D. F. Hayes, *Annu Rev Med.* **2014**, *65*, 95–110.

[4] Z. Altintas, *I. Tothill. Sens. Actuator B-Chem.* **2013**, *188*, 988–98.

[5] S. A. Joosse, T. M. Gorges, K. Pantel. *EMBO Mol Med.* **2015**, *7*, 1–11.

[6] A. Mishra, M. Verma, *Cancers* (Basel) **2010**, *2*, 190–208.

[7] C. S. Dela Cruz, L. T. Tanoue, R. A. Matthay, *Clin. Chest. Med.* **2011**, *32*, 605–644.

[8] S. Mittal, H. Kaur, N. Gautam, A. K. Mantha, *Biosens. Bioelectron.* **2017**, *88*, 217–231.

[9] K. Y. C. Fung, L. Purins, I. K. Priebe, C. Pompeia, G. V. Brierley, B. Tabor, T. Lockett, P. Gibbs, J. Tie, P.

McMurrick, J. Moore, A. Ruszkiewicz, A. Burgess, E. Nice, L. J. Cosgrove, *J. Mol. Biomark Diagn.* **2014**, *S6*, 003.
[10] C. A. K. Borrebaeck, *Nat. Rev. Cancer* **2017**, *17*, 199–204.
[11] G. Ferrín, P. Aguilar-Melero, M. Rodríguez-Perálvarez, J. L. Montero-Álvarez, M. de la Mata, *Hepat. Med.* **2015**, *7*, 1–10.
[12] L. Mi, X. Ji, J. Ji, *Transl. Gastrointest. Cancer* **2016**, *5*, 16–29.
[13] S. Benchimol, A. Fuks, S. Jothy, N. Beauchemin, K. Shirota, C. P. Stanners, *Cell* **1989**, *57*, 327–334.
[14] H. Wang, H. Han, Z. Ma, *Bioelectrochemistry* **2017**, *114*, 48–53.
[15] Y. Zhang, W. Ren, *Anal. Methods* **2013**, *5*, 3379–3385
[16] G.-Z. Li, F. Tian. *Anal. Sci.* **2013**, *29*, 1195–1201.
[17] T. Yu, W. Cheng, Q. Li, C. Luo, L. Yan, D. Zhang, Y. Yin, S. Ding, H. Ju, *Talanta* **2012**, *93*, 433–438.
[18] J. Han, Y. Zhuo, Y. Q. Chai, Y. L. Yuan, R. Yuan, *Biosens. Bioelectron.* **2012**, *31*, 399–405.
[19] Z. Zhong, J. Shan, Z. Zhang, Y. Qing, D. Wang, *Electroanalysis* **2010**, *22*, 2569–2575.
[20] H. Jia, P. Gao, H. Ma, Y. Li, J. Gao, B. Du, Q. Wei, *Talanta* **2015**, *132*, 803–808.
[21] X. Zhang, F. Li, Q. Wei, B. Du, D. Wu, H. Li, *Sens. Actuator B-Chem.* **2014**, *194*, 64–70.
[22] D. Wu, H. Fan, Y. Li, Y. Zhang, H. Liang, Q. Wei, *Biosens. Bioelectron.* **2013**, *46*, 91–96.
[23] H. Ilkhani, A. Ravalli, G. Marrazza, *Chemosensors* **2016**, *4*, 1–10.
[24] E. Arkan, R. Saber, Z. Karimi, M. Shamsipur, *Anal. Chim. Acta.* **2015**, *874*, 66–74.
[25] A. Ravalli, C. G. Rocha, H. Yamanaka, G. Marrazza, *Bioelectrochemistry* **2015**, *106*, 268–275.
[26] S. Patris, P. De Pauw, M. Vandeput, J. Huet, P. V. Antwerpen, S. Muyldermans, J.-M. Kauffmann, *Talanta* **2014**, *130*, 164–170.
[27] R. C. B. Marques, S. Viswanathan, H. P. A. Nouws, C. Delerue-Matos, M. B. Gonzalez-Garcia, *Talanta* **2014**, *129*, 594–599.
[28] M . Emami, M. Shamsipur, R. Saber, R. Irajirad, *Analyst* **2014**, *139*, 2858–2866.
[29] Q. A. M. Al-Khafaji, M. Harris, S. Tombelli, S. Laschi, A. P. F. Turner, M. Mascini, G. Marrazza, *Electroanalysis* **2012**, *24*, 735–742.
[30] S. P. Mucelli, M. Zamuner, M. Tormen, G. Stanta, P. Ugo, *Biosens. Bioelectron.* **2008**, *23*, 1900–1903.
[31] R. Akter, B. Jeong, J.-S. Choi, M. A. Rahman, *Biosens. Bioelectron.* **2016**, *80*, 123–130.
[32] L. Zhao, Q. Wei, H. Wu, J. Dou, H. Li, *Biosens. Bioelectron.* **2014**, *59*, 75–80.
[33] S. Park, A. Singh, S. Kim, H. Yang, *Anal. Chem.* **2014**, *86*, 1560–1566.
[34] C. Li, X. Qiu, K. Deng, Z. Hou, *Anal Methods* **2014**, *6*, 9078–9084.
[35] H. Li, J. He, S. Li, A. P. Turner, *Biosens. Bioelectron.* **2013**, *43*, 25–29.
[36] S. Ge, X. Jiao, D. Chen, *Analyst* **2012**, *137*, 4440–4447.
[37] W. Li, R. Yuan, Y. Chai, Y. Chen, *Biosens. Bioelectron.* **2010**, *25*, 2548–2552.
[38] C. Hong, R. Yuan, Y. Chai, Y. Zhuo, *Anal. Chim. Acta* **2009**, *633*, 244–249.
[39] Y. Yang, Z. Zhong, H. Liu, T. Zhu, J. Wu, M. Li, D. Wang, *Electroanalysis* **2008**, *20*, 2621–2628.
[40] G. Sun, H. Liu, Y. Zhang, J. Yu, M. Yan, X. Song, W. He, *New J. Chem.* **2015**, *39*, 6062–6067.
[41] F. Yang, Z. Yang, Y. Zhuo, Y. Chai, R. Yuan, *Biosens. Bioelectron.* **2015**, *66*, 356–362.
[42] F. Hu, S. Chen, R. Yuan, *Sens. Actuator B-Chem.* **2013**, *176*, 713–722.
[43] Y. Zhuo, R. Yuan, Y. Q. Chai, C. L. Hong, *Analyst* **2010**, *135*, 2036–2042.
[44] Y. Wei, X. Li, X. Sun, H. Ma, Y. Zhang, Q. Wei, *Biosens. Bioelectron.* **2017**, *94*, 141–147.
[45] M. Li, P. Wang, F. Li, Q. Chu, Y. Li, Y. Dong, *Biosens. Bioelectron.* **2017**, *87*, 752–759.
[46] H. Deng, J. Li, Y. Zhang, H. Pan, G. Xu, *Anal. Chim. Acta* **2016**, *926*, 48–54.
[47] H. Ma, Y. Li, Y. Wang, L. Hu, Y. Zhang, D. Fa, T. Yan, Q. Wei, *Biosens. Bioelectron.* **2016**, *78*, 167–173.
[48] Y. Chu, H. Wang, H. Ma, D. Wu, B. Du, Q. Wei, *RSC Adv.* **2016**, *6*, 84698–84704.
[49] J. Biscay, M. B. G. García, A. C. García, *Electroanalysis* **2015**, *27*, 2773–2777.
[50] Y. Wang, Y. Qu, G. Liu, X. Hou, Y. Huang, W. Wu, K. Wu, C. Li, *Microchim. Acta* **2015**, *182*, 2061–2067.
[51] J. Yang, W. Wen, X. Zhang, S. Wang, *Microchim. Acta* **2015**, *182*, 1855–1861.
[52] L. Yang, H. Zhao, G. Deng, X. Ran, Y. Li, X. Xie, C.-P. Li, *RSC Adv.* **2015**, *5*, 74046–74053.
[53] G. Sun, H. Liu, Y. Zhang, J. Yu, M. Yan, X. Song, W. He, *New J. Chem.* **2015**, *39*, 6062–6067.
[54] Y. Huang, Y. Ding, T. Li, M. Yang, *Anal. Methods* **2015**, *7*, 411–415.
[55] J. M. Moon, Y. H. Kim, Y. Cho, *Biosens. Bioelectron.* **2014**, 57, 157–161.
[56] B. Kavosi, A. Salimi, R. Hallaj, K. Amani, *Biosens. Bioelectron.* **2014**, *52*, 20–28.
[57] V. Kumar, S. Srivastava, S. Umrao, R. Kumar, G. Nath, G. Sumana, P. S. Saxena, A. Srivastava, *RSC Adv.* **2014**, *4*, 2267–2273.
[58] L. Ding, J. You, R. Kong, F. Qu, *Anal. Chim. Acta* **2013**, *793*, 19–25.
[59] M. Yan, D. Zang, S. Ge, L. Ge, J. Yu, *Biosens. Bioelectron.* **2012**, *38*, 355–361.
[60] R. Akter, M. A. Rahman, C. K. Rhee, *Anal. Chem.* **2012**, *84*, 6407–6415.
[61] J. Tian, J. Huang, Y. Zhao, S. Zhao, *Microchim. Acta* **2012**, *178*, 81–88.
[62] K. Mao, D. Wu, Y. Li, H. Ma, Z. Ni, Yu H, C. Luo, Q. Wei, B. Du, *Anal Biochem.* **2012**, *422*, 22–27.
[63] M. Yang, A. Javadi, S. Gong, *Sens. Actuator B-Chem.* **2011**, *155*, 357–360.
[64] T. Li, M. Yang, H. Li, *J. Electroanal. Chem.* **2011**, *655*, 50–55.
[65] H. Li, Q. Wei, J. He, T. Li, Y. Zhao, Y. Cai, B. Du, Z. Qian, M. Yang, *Biosens. Bioelectron.* **2011**, *26*, 3590–3595.
[66] Q. Wei, Y. Zhao, C. Xu, D. Wu, Y. Cai, J. He, H. Li, B. Du, M. Yang, *Biosens. Bioelectron.* **2011**, *26*, 3714–3718.
[67] M. Yang, A. Javadi, H. Li, S. Gong, *Biosens. Bioelectron.* **2010**, *26*, 560–565.
[68] B. Qu, L. Guo, X. Chu, D. H. Wu, G. L. Shen, R. Q. Yu, *Anal. Chim. Acta* **2010**, *663*, 147–152.
[69] V. Escamilla-Gomez, D. Hernandez-Santos, M. B. Gonzalez-Garcia, J. M. Pingarron-Carrazon, A. Costa-Garcia, *Biosens. Bioelectron.* **2009**, *24*, 2678–2683.
[70] T. Xua, B. Chia, F. Wub, S. Mab, S. Zhanb, M. Yib, H. Xua, C. Mao, *Biosens. Bioelectron.* **2017**, *95*, 87–93.
[71] T. Xu, B. Chi, J. Gao, M. Chu, W. Fan, M. Yi, H. Xu, C. Mao, *Anal. Chim. Acta* **2017**, *977*, 36–43.
[72] Y. Niu, T. Yang, S. Ma, F. Peng, M. Yi, M. Wan, C. Mao, J. Shen, *Biosens. Bioelectron.* **2017**, *92*, 1–7.
[73] Y. Huang, C. Tang, J. Liu, J. Cheng, Z. Si, T. Li, M. Yang, *Microchim. Acta* **2017**, *184*, 855–861.

[74] H. Wang, Y. Zhang, Y. Wang, H. Ma, B. Du, Q. Wei, *Biosens. Bioelectron.* **2017**, *87*, 745–751.
[75] N. Hui, X. Sun, Z. Song, S. Niu, X. Luo, *Biosens. Bioelectron.* **2016**, *86*, 143–49.
[76] J. Shan, L. Wang, Z. Ma Z, *Sens. Actuator B-Chem.* **2016**, *237*, 666–671.
[77] L. Jiao, Z. Mu, C. Zhu, Q. Wei, H. Li, D. Du, Y. Lin. *Sens. Actuator B-Chem.* **2016**, *231*, 513–519.
[78] Y. Wei, Y. Li, N. Li, Y. Zhang, T. Yan, H. Man, Q. Wei Q, *Biosens. Bioelectron.* **2016**, *79*, 482–487.
[79] Q. Zhai, X. Zhang, J. Li, E. Wang, *Nanoscale* **2016**, *8*, 15303–15308.
[80] L. Jiang, F. Li, J. Feng, P. Wang, Q. Liu, Y. Li, Y. Dong, Q. Wei, *RSC Adv.* **2016**, *6*, 24373–24380.
[81] J. Guo, X. Han, J. Wang, J. Zhao, Z. Guo, Y. Zhang, *Anal. Biochem.* **2015**, *491*, 58–64.
[82] N. Li, H. Ma, W. Cao, D. Wu, T. Yan, B. Du, Q. Wei, *Biosens. Bioelectron.* **2015**, *74*, 786–791.
[83] J. Liu, G. Lin, C. Xiao, Y. Xue, A. Yang, H. Ren, W. Lu, H. Zhao, X. Li, Z. Yuan, *Biosens. Bioelectron.* **2015**, *71*, 82–87.
[84] L. Li, L. Zhang, J. Yu, S. Ge, X. Song, *Biosens. Bioelectron.* **2015**, *71*, 108–114.
[85] F. Li, J. Han, L. Jiang, Y. Wang, Y. Li, Y. Dong, Q. Wei, *Biosens. Bioelectron.* **2015**, *68*, 626–632.
[86] L. Ji, Z. Guo, T. Yan, H. Ma, B. Du, Y. Li, Q. Wei, *Biosens. Bioelectron.* **2015**, *68*, 757–762.
[87] C. Zhou, D. Liu, L. Xu, Q. Li, J. Song, S. Xu, R. Xing, H. Song, *Sci. Rep.* **2015**, *5*, 1–7.
[88] L. Jiang, J. Han, F. Li, J. Gao, Y. Li, Y. Dong, Q. Wei, *Electrochim. Acta* **2015**, *160*, 7–14.
[89] Y. Wang, D. Wu, Y. Zhang, X. Ren, Y. Wang, H. Ma, Q. Wie, *RSC Adv.* **2015**, *5*, 56583–56589.
[90] G. Zhong, R. Lan, W. Zhang, F. Fu, Y. Sun, H. Peng, T. Chen, Y. Cai, A. Liu, J. Lin, X. Lin, *Int. J. Nanomedicine* **2015**, *10*, 2219–2228.
[91] M. C. Tu, H. Y. Chen, Y. Wang, S. M. Moochhala, P. Alagappan, B. Liedberg, *Anal. Chim. Acta* **2015**, *853*, 228–233.
[92] T. Qi, J. Liao, Y. Li, J. Peng, W. Li, B. Chu, H. Li, Y. Wei, Z. Qian, *Biosens. Bioelectron.* **2014**, *61*, 245–250.
[93] Y. Wang, X. Li, W. Cao, Y. Li, H. Li, B. Du, Q Wei, *Talanta* **2014**, *129*, 411–416.
[94] Y. Li, R. Yuan, Y. Chai, Y. Zhuo, H. Su, Y. Zhang, *Microchim. Acta* **2014**, *181*, 679–685.
[95] H. Wang, H. Li, Y. Zhang, Q. Wei, H. Ma, D. Wu, Y. Li, Y. Zhang, B. Du, *Biosens. Bioelectron.* **2014**, *53*, 305–309.
[96] Z. Yang, Y. Chai, R. Yuan, Y. Zhuo, Y. Li, J. Han, N. Liao, *Sens. Actuator B-Chem.* **2014**, *193*, 461–66.
[97] H. P. Peng, Y. Hu, A. L. Liu, W. Chen, X. H. Lin, X.-B. Yu, *J. Electroanal. Chem.* **2014**, *712*, 89–95.
[98] K. Liu, J. Zhang, Q. Liu, H. Huang, *Electrochim. Acta* **2013**, *114*, 448–454.
[99] Q. Gao, J. Han, Z. Ma, *Biosens. Bioelectron.* **2013**, *49*, 323–328.
[100] H. Fan, Z. Guo, L. Gao, Y. Zhang, D. Fan, G. Ji, B. Du, Q. Wei, *Biosens. Bioelectron.* **2015**, *64*, 51–56.
[101] D. Wu, Z. Guo, Y. Liu, A. Guo, W. Lou, D. Fan, Q. Wei, *Talanta* **2015**, *134*, 305–309.
[102] J. Liao, D. Tang, *Curr. Pharm. Anal.* **2009**, *5*, 164–170.
[103] C. Tsé, A. S. Gauchez, W. Jacot, P. J. Lamy, *Cancer Treat. Rev.* **2012**, *38*,133–142.
[104] I. E. Tothill, *Semin. Cell Dev. Biol.* **2009**, *20*, 55–62.
[105] L. Lam, N. McAndrew, M. Yee, T. Fu, J. C. Tchou, H. Zhang, *Biochim. Biophys. Acta* **2012**, *1826*, 199–208.
[106] D. R. Thevenot, K. Tóth, R. A. Durst, G. S. Wilson, *Biosens. Bioelectron.* **2001**, *16*, 121–131.
[107] M. Oliverio, S. Perotto, G. C. Messina, L. Lovato, F. De Angelis, *ACS Appl. Mater. Interfaces* **2017**, *9*, 29394–29411.
[108] L. Tan, Y. Chen, H. Yang, Y. Shi, J. Si, G. Yang, Z. Wu, P. Wang, X. Lu, H. Bai, Y. Yang, *Sens. Actuator B-Chem.* **2009**, *142*, 316–320.
[109] R. I. Jafri, T. Arockiados, N. Rajalakshmi, S. Ramaprabhu, *J. Electrochem. Soc.* **2010**, *157*, B874–B879.
[110] Y. Jung, J. Y. Jeong, B. H. Chung, *Analyst* **2008**, *133*, 697–701.
[111] A. Ulman, *Chem. Rev.* **1996**, *96*, 1533–1554.
[112] N. J. Ronkainen, S. L. Okon, *Materials* **2014**, *7*, 4669–4709.
[113] H. D. Jang, S. K. Kim, H. Chang, J. W. Choi, *Biosens. Bioelectron.* **2015**, *63*, 546–551.
[114] F. Ricci, G. Adornetto, G. Palleschi, *Electrochim. Acta* **2012**, *84*, 74–83.
[115] P. Yáñez-Sedeño, S. Campuzano, J. M. Pingarrón, *Sensors* **2016**, *16*, 1585–1617.
[116] E. Paleček, M. Fojta, *Talanta* **2007**, *74*, 276–290.
[117] V. Mani, B. V. Chikkaveeraiah, J. F. Rusling, *Expert. Opin. Med. Diagn.* **2011**, *5*, 381–391.
[118] R. C. B. Marques, E. Costa-Rama, S. Viswanathan, H. P. A. Nouws, A. Costa-García, C. Delerue-Matos, M. B. González-García, *Sens. Actuator B-Chem.* **2018**, *255*, 918–925.
[119] A. Dasgupta, A. R. Lim, C. M. Ghajar, *Mol. Oncol.* **2017**, *11*, 40–61.
[120] M. Perfézou, A. Turner, A. Merkoçi, *Chem. Soc. Rev.* **2012**, *41*, 2606–2622.
[121] P. T. H. Went, A. Lugli, S. Meier, M. Bundi, M. Mirlacher, G. Sauter, S. Dirnhofer, *Hum. Pathol.* **2004**, *35*, 122–128.
[122] H. Shen, J. Yang, Z. Chen, X. Chen, L. Wang, J. Hu, F. Ji, G. Xie, W. Feng, *Biosens. Bioelectron.* **2016**, *81*, 495–502.
[123] M. Maltez-da Costa, A. Escosura-Muñiz, C. Nogués, L. Barrios, E. Ibáñez, A. Merkoçi, *Nano Lett.* **2012**, *12*, 4164–4171.
[124] Y. Zhuo, R. Yuan, Y. Q. Chai, C. L. Hong, *Anal. Chem.* **2013**, *85*, 1058–1064.
[125] W. Lu, H–Y. Wang, M. Wang, Y. Wang, L. Tao, W. Qian, *RSC Adv.* **2015**, *5*, 24615–24624.

Received: March 9, 2018
Accepted: March 30, 2018
Published online on April 30, 2018